Burst pacemaker activity of the sinoatrial node in sodium–calcium exchanger knockout mice

Angelo G. Torrente[a], Rui Zhang[a], Audrey Zaini[a], Jorge F. Giani[b], Jeanney Kang[a], Scott T. Lamp[a], Kenneth D. Philipson[c], and Joshua I. Goldhaber[a,b,1]

[a]Cedars-Sinai Heart Institute, Los Angeles, CA 90048; [b]Department of Biomedical Sciences, Cedars-Sinai Medical Center, Los Angeles, CA 90048; and [c]Department of Physiology, David Geffen School of Medicine at UCLA, Los Angeles, CA 90095-1751

Edited by Donald M. Bers, University of California, Davis, CA, and accepted by the Editorial Board June 26, 2015 (received for review March 25, 2015)

In sinoatrial node (SAN) cells, electrogenic sodium–calcium exchange (NCX) is the dominant calcium (Ca) efflux mechanism. However, the role of NCX in the generation of SAN automaticity is controversial. To investigate the contribution of NCX to pacemaking in the SAN, we performed optical voltage mapping and high-speed 2D laser scanning confocal microscopy (LSCM) of Ca dynamics in an ex vivo intact SAN/atrial tissue preparation from atrial-specific NCX knockout (KO) mice. These mice lack P waves on electrocardiograms, and isolated NCX KO SAN cells are quiescent. Voltage mapping revealed disorganized and arrhythmic depolarizations within the NCX KO SAN that failed to propagate into the atria. LSCM revealed intermittent bursts of Ca transients. Bursts were accompanied by rising diastolic Ca, culminating in long pauses dominated by Ca waves. The L-type Ca channel agonist BayK8644 reduced the rate of Ca transients and inhibited burst generation in the NCX KO SAN whereas the Ca buffer 1,2-Bis(2-aminophenoxy)ethane-N,N,N′,N′-tetraacetic acid (acetoxymethyl ester) (BAPTA AM) did the opposite. These results suggest that cellular Ca accumulation hinders spontaneous depolarization in the NCX KO SAN, possibly by inhibiting L-type Ca currents. The funny current (I_f) blocker ivabradine also suppressed NCX KO SAN automaticity. We conclude that pacemaker activity is present in the NCX KO SAN, generated by a mechanism that depends upon I_f. However, the absence of NCX-mediated depolarization in combination with impaired Ca efflux results in intermittent bursts of pacemaker activity, reminiscent of human sinus node dysfunction and "tachy-brady" syndrome.

sinoatrial node | sodium-calcium exchange | pacemaker activity | arrhythmia | intracellular calcium

Physiological heart rhythm originates in the sinoatrial node (SAN), a cluster of specialized pacemaker cells located on the endocardial surface of the right atrium (RA). SAN dysfunction (SND) leads to serious arrhythmias characterized by pathological pauses, often alternating with rapid heart rates or atrial fibrillation (1). Each year in the United States, close to 200,000 patients affected with SAN disease require surgical implantation of an electronic pacemaker (2). Therefore, advances in our understanding of SAN pacemaker activity are essential for developing new therapies to avoid this costly procedure and its related morbidity.

In SAN pacemaker cells, action potentials (APs) are thought to be triggered by spontaneous diastolic depolarization (SDD) produced by a coupled system of cellular "clocks" (3). The first clock, known as the "membrane clock," initiates SDD in response to inward funny current (I_f) carried mostly by HCN4 channels (4) although other ion channels, like voltage-dependent Ca channels, have also been implicated (5). The second (and more controversial) clock is referred to as the "Ca clock." This clock produces a depolarizing current in late diastole when local Ca released by ryanodine receptors (RyRs) on the sarcoplasmic reticulum (SR) is extruded by the electrogenic sodium–calcium exchanger (NCX) (3). Both clocks are then synchronized by the opening of L-type Ca channels (LTCCs) during the upstroke of the AP. Ca entry through LTCCs also refills the SR, thereby priming the system for its next release cycle (3).

Several studies have demonstrated the importance of NCX in the mechanism of spontaneous SAN cell depolarization (2, 3, 6–8). However, NCX is also the dominant Ca efflux mechanism in cardiomyocytes (9), and thus an essential mechanism for maintaining cellular Ca balance. How the impairment of Ca efflux could affect SAN automaticity has not been investigated.

To study how NCX contributes to SAN pacemaker activity, we previously created an atrial-specific NCX knockout (KO) mouse, where NCX is totally eliminated from the atria, including the SAN (2). These mice live into adulthood and are healthy despite a lack of P waves on electrocardiogram (ECG). Atrial electrograms (EGMs) are silent, consistent with atrial quiescence, and isolated NCX KO SAN cells lack spontaneous APs despite normal I_f (2). Nevertheless, it is possible to pace the atria and single SAN cells from these mice. Although we found no evidence of spontaneous atrial depolarization in the NCX KO mouse, we did not examine SAN activity directly.

We developed a method for dynamic 2D imaging of intracellular Ca and voltage mapping in the intact explanted mouse SAN. This method takes advantage of the unique properties of the mouse SAN, which is only a few cell layers thick. Using this approach, we found that the intact NCX KO SAN tissue depolarizes spontaneously, contrary to our findings in isolated single cells. However, this pacemaker activity is characterized by bursts of APs alternating with pauses, a pattern reminiscent of the clinical "tachy-brady" syndrome of SND (1). We found that, when intracellular Ca is normal, the complex interplay between I_f and other ion channels is sufficient to generate bursts of APs despite the complete absence of NCX. However, rising

Significance

The sinoatrial node (SAN) generates cardiac pacemaker activity through the interplay of membrane ionic currents and intracellular calcium cycling. SAN dysfunction is a common disorder that usually requires implantation of costly electronic pacemakers. To study the role of intracellular calcium regulation by the sodium/calcium exchanger (NCX) in SAN pacing, we generated an atrial-specific NCX knockout mouse. The SAN beating pattern in these mice is abnormal, with bursts of activity interrupted by frequent pauses reminiscent of clinical SAN disease. We found that cellular calcium accumulation was responsible for this abnormal beating pattern, underscoring the importance of NCX-mediated calcium efflux to normal pacing. We propose that burst firing is a common feature of SAN dysfunction caused by elevated cytoplasmic calcium.

Author contributions: A.G.T., K.D.P., and J.I.G. designed research; A.G.T., R.Z., and J.F.G. performed research; A.G.T., R.Z., A.Z., J.K., S.T.L., and J.I.G. analyzed data; A.G.T., K.D.P., and J.I.G. wrote the paper; J.K. handled mice breeding; and S.T.L. handled optico-electrical engineering.

The authors declare no conflict of interest.

This article is a PNAS Direct Submission. D.M.B. is a guest editor invited by the Editorial Board.

[1]To whom correspondence should be addressed. Email: joshua.goldhaber@cshs.org.

This article contains supporting information online at www.pnas.org/lookup/suppl/doi:10.1073/pnas.1505670112/-/DCSupplemental.

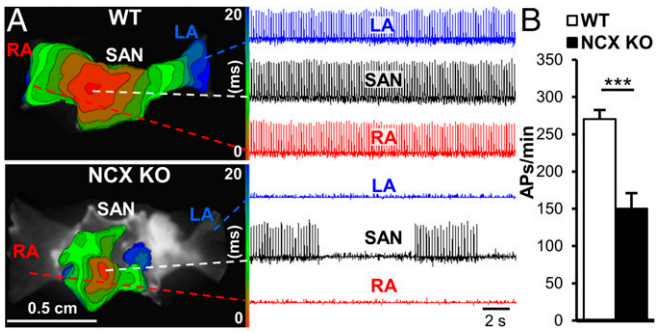

Fig. 1. Optical voltage mapping of explanted SAN/atrial tissue. (*A*) Isochronal voltage maps from WT and NCX KO tissue (*Left*) and corresponding optical recordings of APs from discreet locations (*Right*). (*B*) AP frequency in NCX KO ($n = 11$) and WT tissue ($n = 8$). ***$P < 0.001$, unpaired t test.

intracellular Ca during bursts, combined with the lack of NCX-mediated depolarization, terminates spontaneous pacing. This oscillation of intracellular Ca explains the burst pacing pattern of the NCX KO SAN.

Results

Electrical Activity in the Intact SAN/Atrial Tissue. We dissected and visualized the entire SAN/atrial tissue, including the SAN, RA, and left atrium (LA), using a stereomicroscope with low magnification (7×). In the wild-type (WT), we observed coordinated SAN and atrial contractions (Movie S1). In contrast, NCX KO SANs displayed intermittent contractile activity, and atria were quiescent (Movie S2). To determine whether this mechanical activity was caused by depolarizations, we performed optical voltage mapping. WT tissues exhibited rhythmic APs originating in the SAN (Fig. S1) and spreading synchronously to both atria (Fig. 1*A*). In the NCX KO, we instead recorded bursts of APs originating in the SAN (Fig. S1). Bursts were interrupted by pauses, which significantly reduced the average AP frequency (Fig. 1*B*).

In 6 of 11 NCX KO tissues, electrical activity originating in the SAN did not excite the atria, suggestive of SAN exit block (Fig. 1*A*). In five SANs, we observed partial depolarization of the atria or intermittent conduction block. In those cases where the NCX KO SAN depolarized the atria, conduction velocity was slower than in WT (time from SAN to RA depolarization: KO, 55 ± 2 ms, $n = 4$; WT, 14 ± 1 ms, $n = 6$; $P < 0.001$, unpaired t test). These results explain the lack of P waves on ECG in NCX KO mice.

Because SAN enlargement (WT, 10 ± 1 mm^2, $n = 20$; KO, 14 ± 1 mm^2, $n = 13$; $P < 0.05$, unpaired t test) and atrial remodeling are evident in our NCX KO mouse (Fig. S1) (2), we reasoned that abnormal conduction could be attributed to fibrosis (10, 11) or changes in connexins (Cxs) (12). Indeed, Masson's trichrome stain showed increased fibrosis in the SAN, RA, and LA of NCX KO compared with WT (Fig. S2 *A* and *B*). Quantitative PCR (qPCR) revealed a significant decrease in Cx40 whereas there was no change in Cx45 or Cx43 (Fig. S2*C*).

Ca Transients in the Entire SAN Tissue. To characterize Ca transients in the intact SAN from WT and NCX KO mice, we loaded the SAN/atrial tissue with the Ca dye Cal-520 AM (13) and used high-speed 2D confocal microscopy at physiological temperature to image a large portion of the SAN (14) (Fig. 2 and Movies S3 and S4). In WT, Ca transients occurred simultaneously throughout the SAN (Fig. 2*A*) and were synchronized with contractions (Movie S3). The Ca transient rate (313 ± 12 transients per min, $n = 28$) was comparable with the spontaneous rate of Langendorff perfused hearts (15). Transients had rapid upstrokes (Table S1), consistent with Ca release elicited by depolarization (14). We observed similar Ca transients, synchronized with contractions, in NCX KO SANs (Fig. 2 and Movie S4). However, their firing pattern was characterized by bursts interrupted by pauses, so that the average Ca transient rate (106 ± 8 transients per min, $n = 40$) was reduced compared with WT ($P < 0.001$, unpaired t test). Ca transients in KOs also exhibited a longer time to peak than WT (*Right Insets* of Fig. 2*B* and Table S1). Still, there was no difference in amplitude or decay rate (Table S1), consistent with our observations in paced NCX KO ventricular myocytes (16).

To confirm that the Ca transients described here corresponded to electrical activity, we simultaneously recorded tissue depolarization using three sets of electrodes surrounding the SAN/atrial preparation (Fig. S3*C*). This approach produced bipolar EGMs (17) showing 100% concordance between depolarization and Ca transients in the SAN of both genotypes. EGMs confirmed the absence of electrical activity during pauses in the KO (Fig. S3 *A* and *B*).

In ~80% of NCX KO SAN tissues ($n = 21$ out of 27), we observed low amplitude Ca transients during the decay phase of the preceding transients. These "early aftertransients" (EATs) were suggestive of early afterdepolarizations (EADs) (Fig. S4*A*, red arrows). In contrast, only 14% of WT SANs showed rare EATs. Simultaneous recording of EGMs showed that EATs corresponded to voltage changes. Using optical voltage mapping, we observed events suggestive of EADs (red arrows, Fig. S4*B*) in 75% of NCX KO tissues ($n = 8$) whereas there were none in WT ($n = 8$).

L-Type Ca Current in NCX KO SAN Cells. We previously reported that NCX KO SAN cells have reduced L-type Ca current ($I_{Ca,L}$) amplitude (2). To determine whether Ca-dependent inactivation of $I_{Ca,L}$ is responsible for the reduction in amplitude, we recorded $I_{Ca,L}$ in isolated SAN cells dialyzed with a pipette solution containing either a low or high concentration of the Ca buffer 1,2-Bis(2-aminophenoxy)ethane-N,N,N′,N′-tetraacetic acid (BAPTA, 1 or 10 mM). Under low buffering conditions, the amplitude of

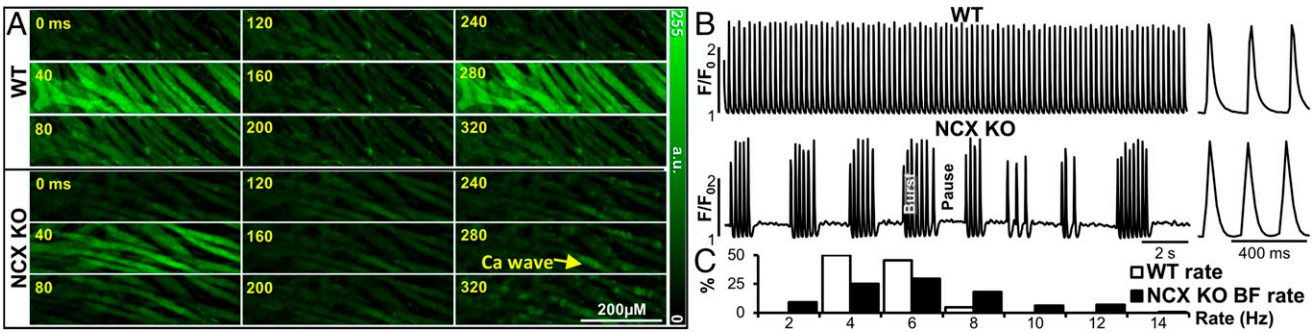

Fig. 2. Ca dynamics in the intact SAN tissue. (*A*) Time series of 2D confocal images of Ca [Cal-520 fluorescence in arbitrary units (a.u.); 50-Hz acquisition speed] in WT and NCX KO SANs. (*B*) Spatial average of fluorescence normalized to baseline (F/F_0) over the entire field of observation in WT and NCX KO SANs. (*Right Insets*) Ca transients on a 400-ms time scale. (*C*) Distribution of Ca transient rates in WT compared with the burst firing (BF) rates in NCX KO.

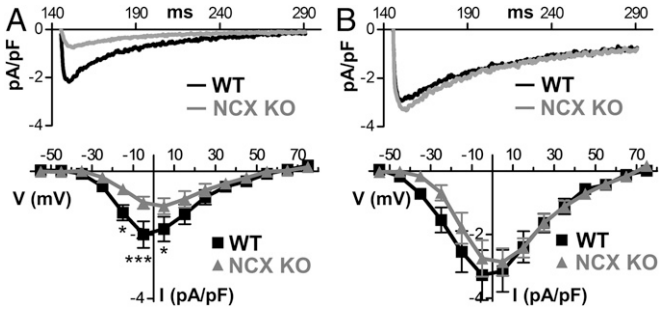

Fig. 3. L-type Ca current ($I_{Ca,L}$) in isolated SAN cells. (*A*) Representative $I_{Ca,L}$ recordings (*Upper*) and average current-voltage plots (*Lower*) from 9 WT (black) and 12 NCX KO (gray) single SAN cells, buffered by a low concentration of BAPTA (1 mM) in the patch pipette. (*B*) $I_{Ca,L}$ recorded under high concentration of BAPTA (10 mM) in WT ($n = 6$) and KO ($n = 7$) SAN cells. ***$P < 0.001$, *$P < 0.05$ by two-way ANOVA with Bonferroni's posttest.

$I_{Ca,L}$ at a test potential of −5 mV was decreased in KO cells by ∼50% compared with WT (Fig. 3*A*), confirming our previous results (2). Under high buffering conditions, $I_{Ca,L}$ was nearly identical in WT and KO (Fig. 3*B*). These findings suggest that $I_{Ca,L}$ reduction in the KO is attributable to Ca-dependent inactivation, likely caused by high subsarcolemmal Ca in the absence of NCX, and similar to our results in ventricular NCX KO cells (18). This reduction in $I_{Ca,L}$ would help to balance cellular Ca, given the reduced Ca efflux capacity in NCX KO SAN, and could also explain the slowed upstroke of Ca transients recorded in KO tissues.

Burst Pattern of Automaticity in NCX KO SAN Tissue. The alternation of bursts and pauses observed in the NCX KO (Fig. 2*B* and Fig. S3*B*) is an unexpected pattern of SAN pacemaking, never observed in WT, and distinct from the arrhythmic bradycardia characterizing most SAN models of impaired depolarization (7, 19, 20). To further investigate this pattern, we defined a burst as any train of three or more Ca transients (21) followed by a pause (14). The average number of Ca transients per burst was 11 ± 1 ($n = 25$ SANs). Bursts (on average, lasting 2.4 ± 0.2 s, $n = 25$ SANs) occupied approximately half of the recording period in NCX KOs whereas the balance consisted of either pauses (lasting 2.1 ± 0.1 s, $n = 25$ SANs) or slow irregular activity (8.1 ± 1.3% of the total recording) (Fig. S4*A*).

As indicated above, the average frequency of Ca transients (including the pauses) in the NCX KO SAN was slower than in the WT. However, the rate of transients within each burst, here indicated as burst-firing (BF) rate (5.7 ± 0.5 Hz, $n = 25$ SANs) (22), was as fast as the rate measured in WT (5.0 ± 0.2 Hz, $n = 22$ SANs; P = NS, by unpaired t test). Nevertheless, the BF rate distribution of NCX KO was wider than the rate distribution in WT and skewed toward higher frequencies, as in tachy-brady syndrome (Fig. 2*C*). In ∼70% of bursts (from 27 NCX KO SANs), there was also a gradual slowing (by 56 ± 3%) of the Ca transient frequency within the burst (Fig. 4 *A* and *B*), a phenomenon reminiscent of spike adaptation in neurons (23, 24).

Intracellular Ca During Spontaneous Bursts and Electrical Stimulation. Previous studies have speculated that dynamic changes in intracellular Ca could cause burst behavior in SAN and neurons (10, 23, 25); however, this concept has not been rigorously tested. In NCX KO SANs, we found that diastolic Ca rose in ∼80% of bursts, either gradually (Fig. 4*A*) or suddenly (Fig. 4*B*). The extent of the Ca increase in these cases was proportional to the BF rate (Fig. 4*D*), and the longest and fastest bursts were associated with the longest pauses (Fig. 4*C*). Copious intracellular Ca waves were always present in confocal recordings during pauses (Fig. 2*A*, Fig. S5, and Movie S4).

Because the rise of Ca in the SAN of NCX KOs correlated with burst termination, we hypothesized that abnormal Ca handling in the absence of NCX might be responsible. To examine this possibility in greater detail, we electrically stimulated both KO and WT SANs at increasing rates (Fig. 5) while recording diastolic Ca. In both WT and KO, faster rates led to proportional increases of diastolic Ca. However, the effect was much more pronounced in KO (Fig. 5 *A* and *B*). We next measured corrected SAN recovery times (cSNRTs) (26) in response to different pacing rates in WT and KO SANs. cSNRT is a common clinical test to investigate SAN dysfunction (27) and is defined as the period of quiescence after rapid pacing, normalized to the pacing rate (11, 26). In both WT and KO, we found that cSNRT was directly proportional to the rate of stimulation (Fig. 5*B*). However, cSNRT was prolonged in the KO compared with WT at all pacing rates tested. The longer cSNRT in KO coincided with the exaggerated increases in diastolic Ca associated with pacing (Fig. 5). Furthermore, return of diastolic Ca to baseline took much longer in NCX KO compared with WT, a phenomenon we also observed during long spontaneous bursts (Fig. 4*C*). These results indicate that the NCX KO SAN has a reduced capacity for recovery after rapid pacing compared with WT, consistent with the absence of NCX-mediated Ca efflux.

Intracellular Ca and Pacemaker Activity of NCX KO SAN. To further investigate the relationship between cell Ca and burst termination, we lowered intracellular Ca using the acetoxymethyl ester (AM) form of the Ca buffer BAPTA. In WT tissues, incubation with a low dose of BAPTA AM (2 μM) for at least 30 min caused a decrease in the average AP rate, consistent with a slowing of SDD as shown previously (28) (Fig. 6 *A* and *B*). However, in NCX KO SANs, we obtained the opposite effect, with a decrease in the period of electrical silence [indicated as quiescent (Q) time] (Fig. 6). Although BAPTA improved NCX KO pacemaker activity by decreasing Q time, it also decreased BF rate in seven of eight NCX KO SANs (Fig. 6*C*).

Next, we increased Ca entry using the LTCC agonist BayK8644 (BayK, 1 μM) (29). BayK caused an increase in Ca transient frequency in WT SAN, consistent with prior studies (6, 19). However, in KO, we obtained the opposite response (Fig. 6 *D* and *E*), with an overall reduction in rate caused by a decrease in the number of bursts and an increase in Q time (Fig. 6*F*). Thus, our results with BayK are the exact opposite of what we obtained with BAPTA, consistent with an inability of NCX KO SANs to cope with additional Ca influx.

NCX KO Pacemaker Activity Is Responsive to I_f Inhibition and β-Adrenergic Stimulation. To investigate the mechanism initiating spontaneous APs in the intact NCX KO SAN, we applied the

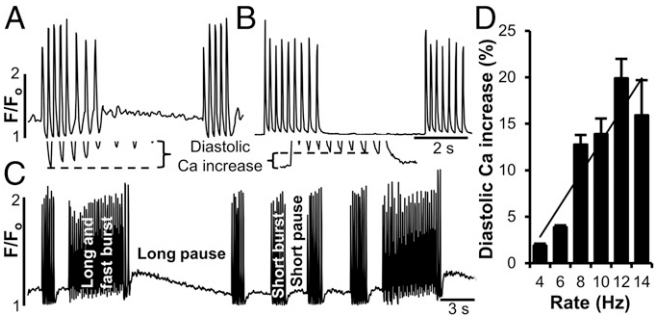

Fig. 4. Diastolic Ca increase and spike adaptation in the NCX KO SAN tissue. Gradual (*A*) and sudden (*B*) increase in diastolic Ca during bursts, followed by gradual (*A*) and rapid (*B*) return to baseline Ca during pauses. *Lower Insets* highlight Ca increase during the first burst in *A* and *B*. Note Ca transients slowing during the bursts (spike adaptation). (*C*) Prolonged bursts with a high burst-firing (BF) rate are associated with higher postburst diastolic Ca and longer pauses compared with the shorter bursts in the tracing. (*D*) Percent increase in diastolic Ca corresponding to BF rate for those spontaneous bursts (∼80% of total) where diastolic Ca increased ($R^2 = 0.82$, $P < 0.01$; $n = 419$ bursts in 25 NCX KO SANs).

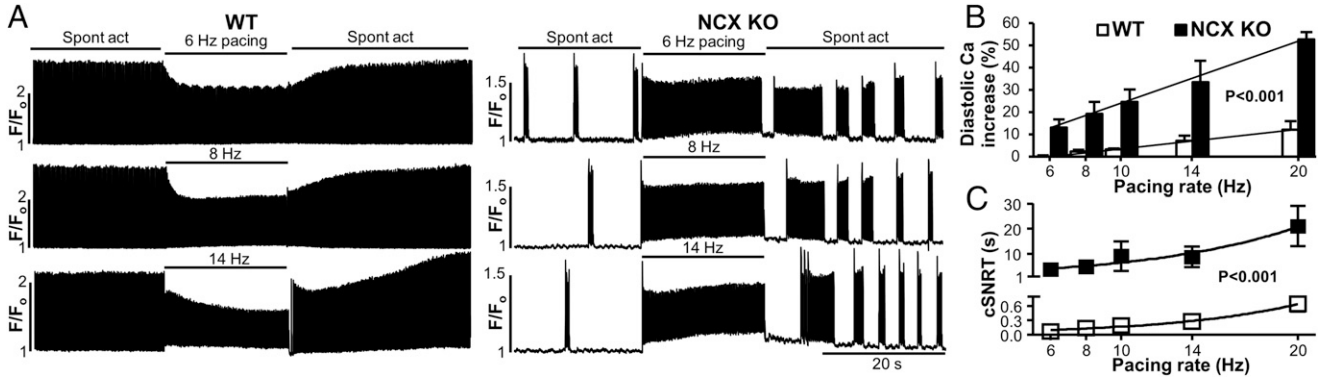

Fig. 5. Diastolic Ca and sinus node recovery time (SNRT) of SAN/atrial tissue. (*A*) Spontaneous Ca transients in WT and NCX KO before and after 20 s of external pacing at 6, 8, and 14 Hz. (*B*) Plot showing the steeper linear rate dependence of diastolic Ca in KO ($n = 4$) compared with WT ($n = 4$). (*C*) Rate dependence and exponential fits of the corrected SNRT (cSNRT) in WT and KO. $P < 0.001$ by two-way ANOVA for WT vs. KO.

specific I_f inhibitor ivabradine (IVA) to WT and KO SAN tissues. IVA (3 μM) caused a significant decrease in the overall rate of Ca transients in both WT and NCX KO (Fig. 7 *A* and *B*), similar to what has been reported previously in normal rabbit SAN tissue (30). In seven of eight NCX KO SANs, the inhibition of I_f not only reduced the BF rate, but also decreased the number of bursts during each recording (Fig. 7 *B* and *C*). Unlike BAPTA AM, which also reduced BF rate, IVA did not decrease Q time, suggesting that IVA suppressed impulse generation without altering cellular Ca.

The β-adrenergic pathway is an essential regulator of SAN pacemaker activity, which also results in Ca loading of the cell by increasing $I_{Ca,L}$ and SR Ca ATPase (SERCA) uptake. β-adrenergic stimulation with isoproterenol (ISO, 1 μM) caused the expected rate increase in WT, but had no effect on the overall rate in NCX KO (Fig. 7 *D* and *E*). However, ISO caused an increase in both BF rate and Q time in 6 out of 11 NCX KO SANs (Fig. 7 *D* and *F*).

Discussion

As the dominant Ca efflux mechanism in cardiomyocytes, NCX ensures Ca balance by removing precisely the amount of Ca that enters the cell with each beat (9). In SAN pacemaker cells, NCX-mediated extrusion of Ca during late diastole also generates a depolarizing current in response to local Ca release by RyRs, a mechanism we and others have previously shown to be important for normal SAN cell automaticity (2, 6, 7). Although the contribution of NCX to late SDD has been widely investigated, less attention has been focused on the importance of NCX-mediated Ca efflux during SAN activity.

We found that the intact NCX KO SAN generated spontaneous APs/Ca transients that were mostly confined to the SAN region. This SAN "exit block" explains why P waves are absent in ECGs recorded from NCX KO mice, which instead display both accelerated and slow junctional rhythm (2). We also found an abnormal pacemaker pattern within the NCX KO SAN, characterized by bursts of transients at a physiological rate interrupted by pauses. This pattern is very different from the bradycardia that typifies most SAN models of impaired depolarization (7, 19, 20). Bursts in the NCX KO SAN led to increased diastolic Ca and Ca waves, consistent with abnormal Ca handling. External pacing led to similar increases in diastolic Ca associated with extremely long cSNRT. Consistent with these findings, Ca buffering with BAPTA AM improved pacemaker activity whereas increased Ca loading with BayK further inhibited it. These results indicate that automaticity in the NCX KO SAN is directly suppressed by impaired Ca efflux. We also found that SAN automaticity was sensitive to the I_f blocker IVA, as well as the β-agonist ISO, confirming the importance of funny channels and cAMP-dependent phosphorylation in SAN pacing, even in the absence of NCX.

Because isolated SAN cells from the NCX KO have no spontaneous APs (2), we were surprised to find any pacemaker activity in the intact SAN. Why single cell activity should differ so

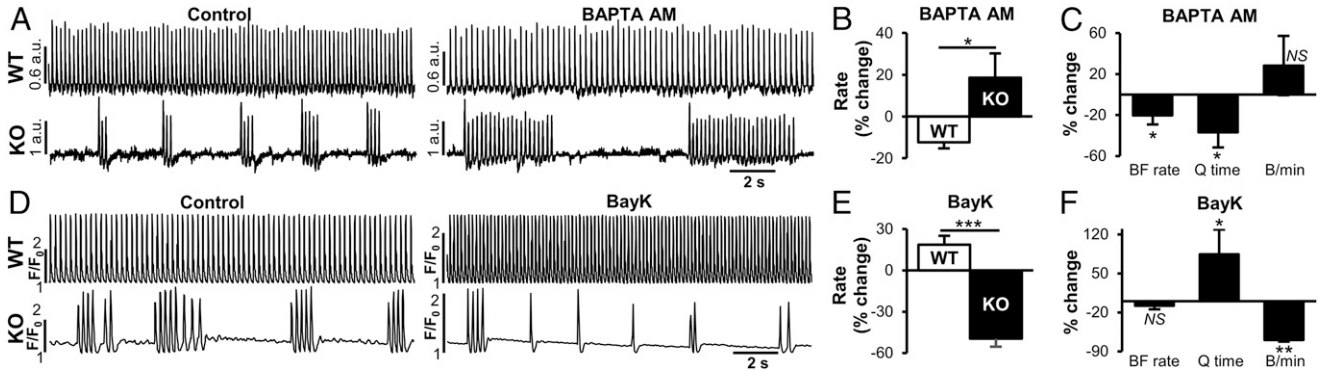

Fig. 6. Intracellular Ca modulation of SAN pacemaker activity. (*A*) Optical recordings of spontaneous APs in WT (*Upper*) and NCX KO (*Lower*) SAN tissue, before (*Left*) and after (*Right*) incubation with BAPTA AM (2 μM). (*B*) Changes in the overall rate of APs in WT ($n = 5$) and NCX KO ($n = 7$) with BAPTA. (*C*) Percent change in burst-firing (BF) rate, quiescent (Q) time and bursts per minute (B/min) in KO SAN ($n = 7$) after incubation with BAPTA. (*D*) Confocal recordings of Ca transients in WT (*Upper*) and NCX KO (*Lower*) SAN tissue, before (*Left*) and after (*Right*) perfusion with BayK (1 μM). (*E*) Changes in the overall rate of transients in WT ($n = 7$) and NCX KO ($n = 6$) with BayK. (*F*) Percent change, same parameters as in *C*, but in response to BayK. $*P < 0.05$, $**P < 0.01$, $***P < 0.001$, unpaired *t* test.

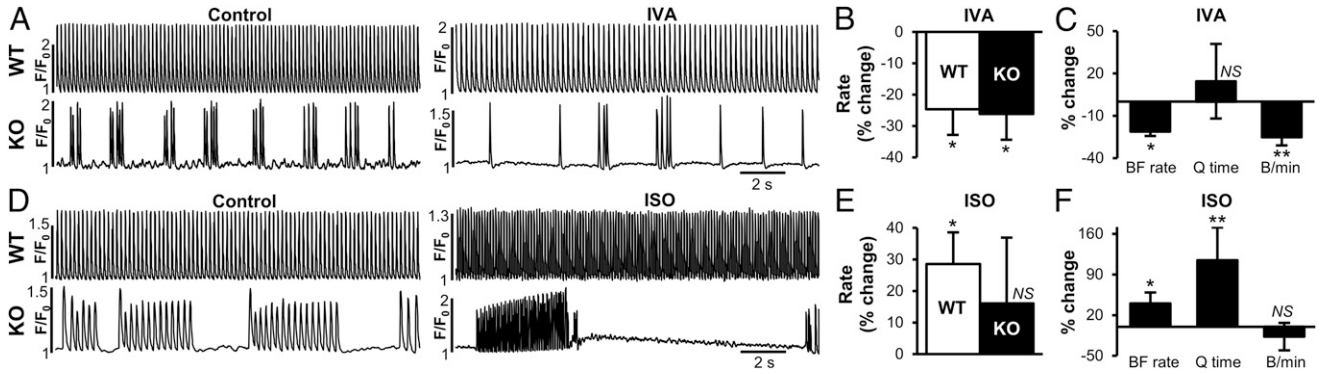

Fig. 7. I_f and β-adrenergic modulation of SAN pacemaker activity. (*A*) Confocal recordings of spontaneous Ca transients in a WT (*Upper*) and NCX KO (*Lower*) SAN, before (*Left*) and after (*Right*) perfusion with ivabradine (IVA, 3μM). (*B*) Changes in the overall rate of Ca transients in WT ($n = 6$) and NCX KO ($n = 8$) with IVA. (*C*) Percent change in burst-firing (BF) rate, quiescent time (Q) time, and bursts per minute (B/min) in NCX KO SAN tissue ($n = 7$) after IVA. (*D*) Spontaneous Ca transients in WT (*Upper*) and NCX KO (*Lower*) SAN tissue, before (*Left*) and after (*Right*) stimulation with ISO (1 μM). (*E*) Changes in the overall rate of Ca transients in WT ($n = 5$) and NCX KO ($n = 11$) with ISO. (*F*) Percent change in the same parameters as in *C* for the 6 NCX KO tissues (out of 11 tested) clearly responding to ISO (1 μM). $*P < 0.05$, $**P < 0.01$, unpaired *t* test.

much from tissue behavior is uncertain, but such differences have been described in other organs such as pancreas (31). A similar mismatch between single cell and SAN tissue behavior has been described in a tamoxifen-induced HCN4 KO mouse (32). In our previous study (2), isolated NCX KO SAN cells had normal diastolic Ca, likely because these cells were electrically silent. Further study will be needed to explain the different behavior in cells and tissue, but we speculate that the more physiological cellular network of the intact SAN reinforces I_f-mediated depolarization.

Our results differ somewhat from the two other mouse models of NCX KO SAN (6, 7). Both of these models exhibit a much less severe phenotype in SAN cell function than our mice (2), which may be due to incomplete ablation of NCX. Nevertheless, there are certain similarities: Gao et al. (6) showed an impaired response to ISO and Bay K, as we did; Herrmann et al. (7) reported bursts alternating with pauses in ECG traces, comparable with our NCX KO SAN pattern.

Impaired Conduction to the Atria. Voltage mapping in the NCX KO SAN revealed disorganized depolarizations, along with delayed or blocked conduction to the atria. There are several potential explanations for abnormal atrial conduction. Atrial remodeling occurs in our NCX KO mice (2), and we found that atrial fibrosis is increased compared with WT (Fig. S2). Fibrosis could interfere with conduction between myocytes (10), particularly in the setting of Cx40 reduction (Fig. S2). The cause of increased fibrosis in the atria of these mice is uncertain, but Ca overload has been implicated in the activation of apoptotic pathways in myocytes leading to fibrosis (11). A similar etiology has been suggested for the fibrotic changes and disordered conduction in the SAN and atria of calsequestrin KO ($Casq2^{-/-}$) mice (10). Whether Ca loading is also responsible for the decreased Cx40 in NCX KO atria is uncertain. However, Cx40 ablation is known to impair SAN/atria conduction (12). Loss of SAN cells through apoptosis in the NCX KO tissue, combined with the atrial enlargement, could also increase source/sink mismatch (11), thereby restricting spread of conduction to the atria.

Ca Accumulation in the NCX KO SAN. In the absence of NCX, Ca removal is mediated by the only alternative Ca efflux mechanism, the plasma membrane Ca pump (PMCA) (33). Although this protein is highly expressed in NCX KO atria (2), it is a much slower transport mechanism compared with NCX. Thus, it is not surprising that bursts of spontaneous pacemaker activity in the KO led to significant increases in diastolic Ca followed by Ca waves and cessation of automaticity. Spontaneous automaticity returned once Ca recovered to baseline, presumably through the activity of PMCA. External pacing in the NCX KO SAN effectively resulted in the same response: a significant increase in diastolic Ca associated with an extremely long cSNRT compared with WT. The duration of the cSNRT was directly proportional to the pacing rate and consequent level of Ca accumulation. Presumably the increased diastolic Ca further inactivated an already compromised $I_{Ca,L}$ in the KO SAN or, less likely, in latent extranodal pacemakers, thus contributing to the prolonged cSNRT by inhibiting depolarization. $I_{Ca,L}$ inactivation by elevated diastolic Ca is also thought to cause pauses in $RyR2^{R4496C}$ mice (14), a model of catecholaminergic polymorphic ventricular tachycardia (CPVT). Bursts of pacemaker activity followed by pauses, associated with a rise and fall of Ca, have also been observed in the SANs of another CPVT model, $Casq2^{-/-}$ mice (10). These mice have abnormal SR Ca release and periods of elevated diastolic Ca corresponding to pauses. Finally, SAN cells isolated from heterozygous ankyrin-B KO mice, which have reduced NCX and $Ca_v1.3$ expression, also show a burst pattern attributed to impaired Ca homeostasis (34). Thus, burst firing seems to be a common feature caused by elevated cytoplasmic Ca and compromised $I_{Ca,L}$. Possibly $Ca_v1.3$ is also decreased in NCX KO although macroscopic I_{Ca} is fully restored by Ca buffering with BAPTA.

Both WT and NCX KO transiently accelerated their spontaneous rate after external pacing (Fig. 5*A*). We speculate that this increased rate may be a consequence of activation of the adenylate/cAMP pathway by Ca (35).

Similar to $RyR2^{R4496C}$ mice, $I_{Ca,L}$ was reduced at baseline in NCX KO SAN cells. This decrease in $I_{Ca,L}$ could be mitigated by buffering intracellular Ca with BAPTA, a response we have also observed in isolated NCX KO ventricular myocytes (18). Because buffering intracellular Ca in single patch-clamped SAN cells could restore $I_{Ca,L}$, we tried the same approach in intact SAN tissue using the cell permeable Ca buffer, BAPTA AM. This treatment improved SAN pacemaker activity in the NCX KO by decreasing quiescent time. Conversely, increasing Ca entry using the LTCC agonist BayK suppressed NCX KO pacemaker activity by increasing quiescent time. β-adrenergic stimulation of NCX KO SAN with ISO increased the rate during the burst (BF rate) but, paradoxically, reduced overall rate because of increased Ca loading and consequent prolonged quiescent time (Fig. 7*D*).

Parallel Mechanisms Between NCX KO Pacemaker Activity and Burst Firing in Neurons and Chromaffin Cells. Burst firing is a common property of different cell types, including pancreatic islet cells (31), chromaffin cells (36), and several types of neurons (29, 37, 38), but, to our knowledge, it has not been studied in the SAN. Burst-firing activity can occur in neurons during normal physiological function (38), after pharmacological stimulation (37), or as a consequence of Parkinson's disease (39). In these systems, Ca modulation of specific ion channels [e.g., $I_{Ca,L}$, Small K (SK), Big K (BK)] causes

burst termination (29, 36–38) whereas Ca-activated transient receptor potential melastatin (TRPM) channels (29, 40) are important for maintaining burst firing. Similar to our findings in the NCX KO SAN, buffering intracellular Ca in neuronal systems can alter burst firing (37).

In the NCX KO SAN, we found that the frequency of Ca transients during bursts gradually slowed until burst termination (Fig. 4). This slowing is reminiscent of spike adaptation (23, 24), a phenomenon well-described in neuronal and chromaffin cells and thought to be caused by activation of Ca-dependent K currents (22, 23, 36). Big K (41) and TRPM4 channels (40) are present in the SAN, and SAN dysfunction occurs after ablation of Small K channels (42). Thus, NCX KO SAN burst firing may be modulated by the same Ca-activated channels found in neurons and chromaffin cells. Ca activation of TRPM4 channels may also contribute to the EADs we recorded in the NCX KO SAN preparation (43).

Conclusion

Despite the lack of NCX-mediated spontaneous diastolic depolarization (i.e., a broken Ca clock), we found that I_f and $I_{Ca,L}$ are capable of initiating bursts of APs in the SAN of atrial-specific NCX KO mice. Our results suggest that, in the absence of NCX-mediated Ca efflux, Ca entry during APs accumulates until the level is sufficiently high to terminate the burst. This termination is likely mediated in part by Ca-dependent inactivation of $I_{Ca,L}$. Other Ca-activated repolarizing currents (e.g., SK or BK) (41, 42) may also contribute to burst termination although this possibility was not tested.

In conclusion, our results suggest a new mechanism of pacemaker dysfunction caused by NCX ablation and consequent impaired Ca efflux. This mechanism is complementary to the impairment of SDD caused by the absence of NCX-mediated depolarization. Our study also highlights a remarkably common Ca-dependent burst-firing behavior that is present in both neurons and dysfunctional SAN, with many similarities to the clinical tachy-brady syndrome (1).

Methods

Detailed methods can be found in *SI Methods*. All animal procedures were reviewed and approved by the Institutional Animal Care and Use Committee of Cedars-Sinai Medical Center.

ACKNOWLEDGMENTS. We thank E. Marban, K. Bernstein, and M. Ottolia for sharing laboratory equipment and for helpful discussion. This work was performed during A.G.T.'s tenure of "The Heart Rhythm Society Fellowship in Cardiac Pacing and Electrophysiology." This work was supported by American Heart Association/National Grant 12IRG9140020 (to J.I.G.), NIH Grant R01HL04509 (to J.I.G. and K.D.P.), NIH Grant R01HL70828 (to J.I.G.), and the Heart Rhythm Society (A.G.T.).

1. Semelka M, Gera J, Usman S (2013) Sick sinus syndrome: A review. *Am Fam Physician* 87(10):691–696.
2. Groenke S, et al. (2013) Complete atrial-specific knockout of sodium-calcium exchange eliminates sinoatrial node pacemaker activity. *PLoS One* 8(11):e81633.
3. Lakatta EG, Maltsev VA, Vinogradova TM (2010) A coupled SYSTEM of intracellular Ca2+ clocks and surface membrane voltage clocks controls the timekeeping mechanism of the heart's pacemaker. *Circ Res* 106(4):659–673.
4. Severi S, Fantini M, Charawi LA, DiFrancesco D (2012) An updated computational model of rabbit sinoatrial action potential to investigate the mechanisms of heart rate modulation. *J Physiol* 590(Pt 18):4483–4499.
5. Mangoni ME, Nargeot J (2008) Genesis and regulation of the heart automaticity. *Physiol Rev* 88(3):919–982.
6. Gao Z, et al. (2013) Genetic inhibition of Na+-Ca2+ exchanger current disables fight or flight sinoatrial node activity without affecting resting heart rate. *Circ Res* 112(2):309–317.
7. Herrmann S, et al. (2013) The cardiac sodium-calcium exchanger NCX1 is a key player in the initiation and maintenance of a stable heart rhythm. *Cardiovasc Res* 99(4):780–788.
8. Sanders L, Rakovic S, Lowe M, Mattick PA, Terrar DA (2006) Fundamental importance of Na+-Ca2+ exchange for the pacemaking mechanism in guinea-pig sino-atrial node. *J Physiol* 571(Pt 3):639–649.
9. Ottolia M, Torres N, Bridge JH, Philipson KD, Goldhaber JI (2013) Na/Ca exchange and contraction of the heart. *J Mol Cell Cardiol* 61:28–33.
10. Glukhov AV, et al. (2015) Calsequestrin 2 deletion causes sinoatrial node dysfunction and atrial arrhythmias associated with altered sarcoplasmic reticulum calcium cycling and degenerative fibrosis within the mouse atrial pacemaker complex1. *Eur Heart J* 36(11):686–697.
11. Swaminathan PD, et al. (2011) Oxidized CaMKII causes cardiac sinus node dysfunction in mice. *J Clin Invest* 121(8):3277–3288.
12. Hagendorff A, Schumacher B, Kirchhoff S, Lüderitz B, Willecke K (1999) Conduction disturbances and increased atrial vulnerability in Connexin40-deficient mice analyzed by transesophageal stimulation. *Circulation* 99(11):1508–1515.
13. Tada M, Takeuchi A, Hashizume M, Kitamura K, Kano M (2014) A highly sensitive fluorescent indicator dye for calcium imaging of neural activity in vitro and in vivo. *Eur J Neurosci* 39(11):1720–1728.
14. Neco P, et al. (2012) Paradoxical effect of increased diastolic Ca(2+) release and decreased sinoatrial node activity in a mouse model of catecholaminergic polymorphic ventricular tachycardia. *Circulation* 126(4):392–401.
15. Glukhov AV, Fedorov VV, Anderson ME, Mohler PJ, Efimov IR (2010) Functional anatomy of the murine sinus node: High-resolution optical mapping of ankyrin-B heterozygous mice. *Am J Physiol Heart Circ Physiol* 299(2):H482–H491.
16. Henderson SA, et al. (2004) Functional adult myocardium in the absence of Na^+-Ca^{2+} exchange: Cardiac-specific knockout of NCX1. *Circ Res* 95(6):604–611.
17. Fedorov VV, Hucker WJ, Dobrzynski H, Rosenshtraukh LV, Efimov IR (2006) Postganglionic nerve stimulation induces temporal inhibition of excitability in rabbit sinoatrial node. *Am J Physiol Heart Circ Physiol* 291(2):H612–H623.
18. Pott C, Yip M, Goldhaber JI, Philipson KD (2007) Regulation of cardiac L-type Ca2+ current in Na+-Ca2+ exchanger knockout mice: Functional coupling of the Ca2+ channel and the Na+-Ca2+ exchanger. *Biophys J* 92(4):1431–1437.
19. Mangoni ME, et al. (2003) Functional role of L-type Cav1.3 Ca2+ channels in cardiac pacemaker activity. *Proc Natl Acad Sci USA* 100(9):5543–5548.
20. Baruscotti M, et al. (2011) Deep bradycardia and heart block caused by inducible cardiac-specific knockout of the pacemaker channel gene Hcn4. *Proc Natl Acad Sci USA* 108(4):1705–1710.
21. Johnson SW, Wu YN (2004) Multiple mechanisms underlie burst firing in rat midbrain dopamine neurons in vitro. *Brain Res* 1019(1-2):293–296.
22. Grace AA, Bunney BS (1984) The control of firing pattern in nigral dopamine neurons: Burst firing. *J Neurosci* 4(11):2877–2890.
23. Engel J, Schultens HA, Schild D (1999) Small conductance potassium channels cause an activity-dependent spike frequency adaptation and make the transfer function of neurons logarithmic. *Biophys J* 76(3):1310–1319.
24. Del Negro CA, Hsiao CF, Chandler SH, Garfinkel A (1998) Evidence for a novel bursting mechanism in rodent trigeminal neurons. *Biophys J* 75(1):174–182.
25. Richter DW, Champagnat J, Jacquin T, Benacka R (1993) Calcium currents and calcium-dependent potassium currents in mammalian medullary respiratory neurones. *J Physiol* 470:23–33.
26. Lou Q, et al. (2013) Tachy-brady arrhythmias: The critical role of adenosine-induced sinoatrial conduction block in post-tachycardia pauses. *Heart Rhythm* 10(1):110–118.
27. Asseman P, et al. (1991) Postextrasystolic sinoatrial exit block in human sick sinus syndrome: Demonstration by direct recording of sinus node electrograms. *Am Heart J* 122(6):1633–1643.
28. Capel RA, Terrar DA (2015) Cytosolic calcium ions exert a major influence on the firing rate and maintenance of pacemaker activity in guinea-pig sinus node. *Front Physiol* 6:23.
29. Lee CR, Machold RP, Witkovsky P, Rice ME (2013) TRPM2 channels are required for NMDA-induced burst firing and contribute to H(2)O(2)-dependent modulation in substantia nigra pars reticulata GABAergic neurons. *J Neurosci* 33(3):1157–1168.
30. Thollon C, et al. (1994) Electrophysiological effects of S 16257, a novel sino-atrial node modulator, on rabbit and guinea-pig cardiac preparations: comparison with UL-FS 49. *Br J Pharmacol* 112(1):37–42.
31. Smolen P, Rinzel J, Sherman A (1993) Why pancreatic islets burst but single beta cells do not: The heterogeneity hypothesis. *Biophys J* 64(6):1668–1680.
32. Herrmann S, Stieber J, Stöckl G, Hofmann F, Ludwig A (2007) HCN4 provides a 'depolarization reserve' and is not required for heart rate acceleration in mice. *EMBO J* 26(21):4423–4432.
33. Oceandy D, Stanley PJ, Cartwright EJ, Neyses L (2007) The regulatory function of plasma-membrane Ca(2+)-ATPase (PMCA) in the heart. *Biochem Soc Trans* 35(Pt 5):927–930.
34. Le Scouarnec S, et al. (2008) Dysfunction in ankyrin-B-dependent ion channel and transporter targeting causes human sinus node disease. *Proc Natl Acad Sci USA* 105(40):15617–15622.
35. Younes A, et al. (2008) Ca(2+) -stimulated basal adenylyl cyclase activity localization in membrane lipid microdomains of cardiac sinoatrial nodal pacemaker cells. *J Biol Chem* 283(21):14461–14468.
36. Vandael DH, Zuccotti A, Striessnig J, Carbone E (2012) Ca(V)1.3-driven SK channel activation regulates pacemaking and spike frequency adaptation in mouse chromaffin cells. *J Neurosci* 32(46):16345–16359.
37. Mrejeru A, Wei A, Ramirez JM (2011) Calcium-activated non-selective cation currents are involved in generation of tonic and bursting activity in dopamine neurons of the substantia nigra pars compacta. *J Physiol* 589(Pt 10):2497–2514.
38. Pace RW, Mackay DD, Feldman JL, Del Negro CA (2007) Inspiratory bursts in the preBötzinger complex depend on a calcium-activated non-specific cation current linked to glutamate receptors in neonatal mice. *J Physiol* 582(Pt 1):113–125.
39. Ibáñez-Sandoval O, et al. (2007) Bursting in substantia nigra pars reticulata neurons in vitro: Possible relevance for Parkinson disease. *J Neurophysiol* 98(4):2311–2323.
40. Hof T, Simard C, Rouet R, Sallé L, Guinamard R (2013) Implication of the TRPM4 non-selective cation channel in mammalian sinus rhythm. *Heart Rhythm* 10(11):1683–1689.
41. Lai MH, et al. (2014) BK channels regulate sinoatrial node firing rate and cardiac pacing in vivo. *Am J Physiol Heart Circ Physiol* 307(9):H1327–H1338.
42. Zhang Q, et al. (2008) Functional roles of a Ca2+-activated K+ channel in atrioventricular nodes. *Circ Res* 102(4):465–471.
43. Simard C, Hof T, Keddache Z, Launay P, Guinamard R (2013) The TRPM4 non-selective cation channel contributes to the mammalian atrial action potential. *J Mol Cell Cardiol* 59:11–19.